

## Electronic Supplementary Information

### Site-projected electronic structure of two-dimensional $\text{Ti}_3\text{C}_2$ MXene: role of the surface functionalization groups

D. Magne,<sup>a</sup> V. Mauchamp,<sup>\*a</sup> S. Célérier,<sup>b</sup> P. Chartier,<sup>a</sup> and T. Cabioc'h<sup>a</sup>

<sup>a</sup> Institut Pprime, UPR 3346 CNRS - Université de Poitiers - ISAE-ENSMA, BP 30179, 86962 Futuroscope-Chasseneuil Cedex, France.

<sup>b</sup> Institut de Chimie des Milieux et Matériaux de Poitiers (IC2MP), Université de Poitiers, CNRS, F-86073 Poitiers, France.

\* email: vincent.mauchamp@univ-poitiers.fr

## 1 Synthesis and characterization of the $\text{Ti}_3\text{C}_2\text{T}_x$ powders

**Synthesis of  $\text{Ti}_3\text{AlC}_2$**  The  $\text{Ti}_3\text{AlC}_2$  powders, used as precursors to obtain the  $\text{Ti}_3\text{C}_2\text{T}_x$ , were synthesized by pressureless sintering ( $1450\text{ }^\circ\text{C}$ /two hours) of TiC, Ti and Al powders mixed in proportions matching the desired composition of the MAX phase. This procedure results in a  $\text{Ti}_3\text{AlC}_2$  porous sample, almost pure from the X-ray diffraction point of view as evidenced by figure S1.

**Synthesis of  $\text{Ti}_3\text{C}_2\text{T}_x$  using HF** 21 mL of aqueous HF (Sigma-Aldrich,  $\geq 48\%$ ) were introduced in a plastic vessel containing 2g of  $\text{Ti}_3\text{AlC}_2$  (initial particles sizes lower than  $25\text{ }\mu\text{m}$  obtained after sieving). The exfoliation of aluminum was performed at room temperature during 24h. The resulting suspension was filtered (PVDF membrane,  $0.22\text{ }\mu\text{m}$  pore size) and washed several times with deionized water. The obtained powders were dried at  $80\text{ }^\circ\text{C}$  during 24h.

**Synthesis of  $\text{Ti}_3\text{C}_2\text{T}_x$  using LiF/HCl** This synthesis method is partly based on the work of Ghidiu *et al.*:<sup>[1]</sup> 1 g of LiF (Aldrich,  $\geq 99.0\%$ ) were added to 20 mL of HCl 7M (prepared from HCl 37% - Sigma-Aldrich) and stirred during 30 min. Then, 1.5g of  $\text{Ti}_3\text{AlC}_2$  powder ( $\leq 25\text{ }\mu\text{m}$ ) were introduced in this solution progressively to avoid initial overheating, the reaction being exothermic. This mixture was heated at  $60\text{ }^\circ\text{C}$  during 90 h and the suspension was filtered, washed and dried as described for the HF exfoliation.

**X-ray diffractograms** XRD analysis of the powders was carried out on a PANalytical EMPYREAN powder diffractometer using  $\text{CuK}_\alpha$  radiation source ( $\text{K}_{\alpha 1} = 1.5406\text{ \AA}$  and  $\text{K}_{\alpha 2} = 1.5444\text{ \AA}$ ). These patterns were collected with a  $0.07^\circ$  step and 420 s dwell time. Phase identification of  $\text{TiOF}_2$  and  $\text{Ti}_3\text{AlC}_2$  was performed with the HighScorePlus software (PANalytical©) and by comparison with the ICDD database reference files. The resulting X-ray diffraction (XRD) patterns obtained for each etching environment are compared with the XRD pattern of the initial  $\text{Ti}_3\text{AlC}_2$  powder in Fig. S1. After etching, the initial MAX phase disappear entirely for both etching methods, confirming the total etching of the aluminium and the formation of the MXene phase. A drastic

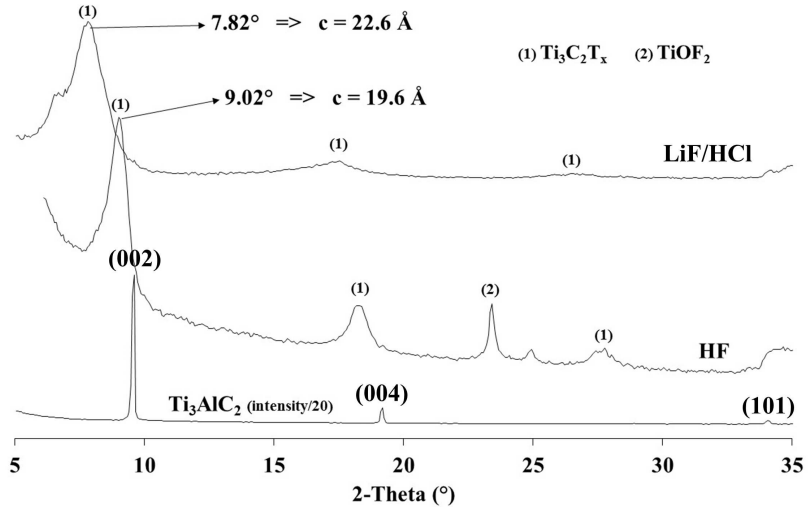


Figure S1: X-ray diffractograms of (bottom) the  $\text{Ti}_3\text{AlC}_2$  powder, (middle) HF-prepared and (top) LiF/HCl-prepared  $\text{Ti}_3\text{C}_2\text{T}_x$  powders.

loss in crystallinity is also evidenced. The XRD pattern of  $\text{Ti}_3\text{C}_2\text{T}_x$  (HF) is similar to those reported previously in the literature and prepared in the same conditions.[2] The (002) peak of the initial MAX phase is shifted to lower angles ( $9.02^\circ$ ) indicating a higher  $c$  parameter ( $19.6 \text{ \AA}$ ).[2] On this sample,  $\text{TiOF}_2$  is also evidenced as a secondary phase. This phase, already observed sometimes with HF, is probably formed due to the harsh environment (aqueous HF). For  $\text{Ti}_3\text{C}_2\text{T}_x$  (LiF/HCl), this secondary phase was not observed, this medium being less aggressive. Interestingly, the (002) peak shifted at  $7.82^\circ$  corresponding to  $c = 22.6 \text{ \AA}$ , which is higher than the  $c$  of  $\text{Ti}_3\text{C}_2\text{T}_x$  (HF). This is probably due to the insertion of water between the sheets as explained by Ghidiu *et al.*[1]

**SEM and TEM characterizations** The  $\text{Ti}_3\text{C}_2\text{T}_x$  powders were characterized by Scanning Electron Microscopy (SEM) using a JEOL Field Emission Gun 7001F-TTLS electron microscope. The corresponding SEM micrographs, recorded in backscattered electrons mode, are given in figure S3 [a] and [b] for the HF and LiF/HCl-prepared samples respectively. These micrographs, very similar to others previously reported in the literature, clearly show the successful exfoliation of the MAX phase resulting in the stacking of 2D  $\text{Ti}_3\text{C}_2\text{T}_x$  sheets, with a more compacted stack for the samples prepared with LiF/HCl as generally observed for such samples.[1] The synthesis of the MXene have been further confirmed by transmission electron microscopy experiments performed on a JEOL 2200FS. The selected area electron diffraction patterns (not shown here) confirm the hexagonal-like structure in the basal plane with unit cell parameters in very good agreement with those reported from XRD data. More important, the complete exfoliation of the sampled areas have been systematically checked by recording the bulk plasmon (BP) using EELS (see Fig. S3 [c]): this signature is a very convenient evidence of the exfoliation since the BP is shifted from 20.5 eV for  $\text{Ti}_3\text{AlC}_2$  to 23.5 eV for the  $\text{Ti}_3\text{C}_2\text{T}_x$ .[5] This last energy

is identical to the BP energy of TiC as discussed in ref. [4].

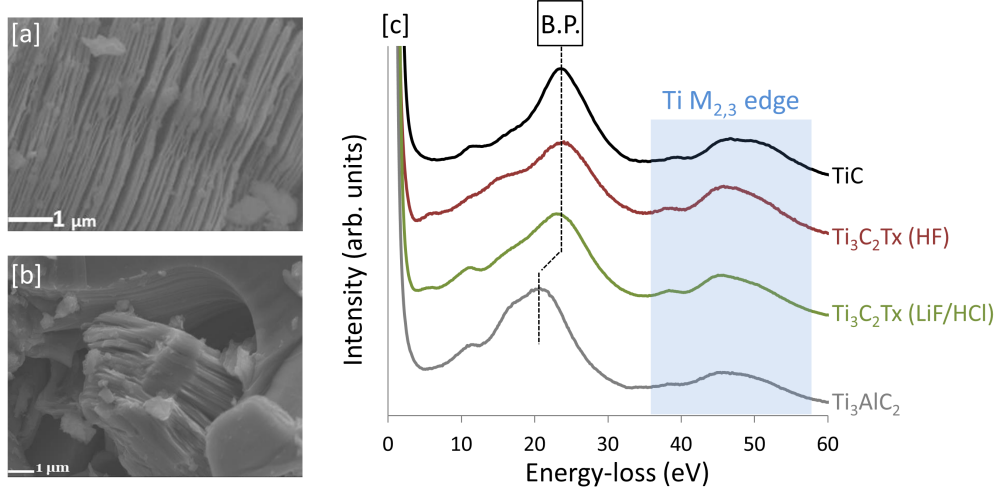


Figure S2: SEM micrographs in backscattered electrons mode of the (a) HF and (b) LiF/HCl-prepared  $\text{Ti}_3\text{C}_2\text{T}_x$  powders. (c) Typical valence electron energy-loss spectra recorded on  $\text{Ti}_3\text{AlC}_2$ ,  $\text{Ti}_3\text{C}_2\text{T}_x$ -LiF/HCl,  $\text{Ti}_3\text{C}_2\text{T}_x$ -HF and a reference TiC sample. The shift of the bulk plasmon (BP), characteristic of the exfoliation, is evidenced. Lines are given as guides to the eyes.

## 2 Simulation of the core-loss spectra

As mentioned in the paper, the C and F-K edges were computed using the site and symmetry projected unoccupied densities of states of the F and C atoms computed in a PAW-based approach. In a single particle framework, such calculations mainly involve three approximations:

- (i) ignoring the role of the matrix elements in equation (1) of the paper
- (ii) treating the core-hole effect in the Z+1 approximation instead of considering the relaxation of the electronic structure due to the removal of a  $1s$  electron on the excited atom
- (iii) treating the electron/ion interactions in the PAW formalism

These approximations have been checked to have a negligible effect on the simulations by computing the exact electron inelastic cross section using an all electron/full potential approach based on the (L)APW formalism. Such calculations were performed with the WIEN2k code and its TELNES extension on the C-K edge of one carbon atom in the  $\text{Ti}_3\text{C}_2\text{F}_2$  system.[3, 4] The following parameters have been used for the calculations:

- the muffin-tin radii were fixed to 1.74, 2.07 and 1.97 bohr for the Ti, C and F atoms respectively

- the basis set size was fixed to  $RK_{max} = 7.5$
- a  $21 \times 21 \times 2$  Monkhorst Pack k-point mesh in the first Brillouin zone was used for the computation of the inelastic cross-section

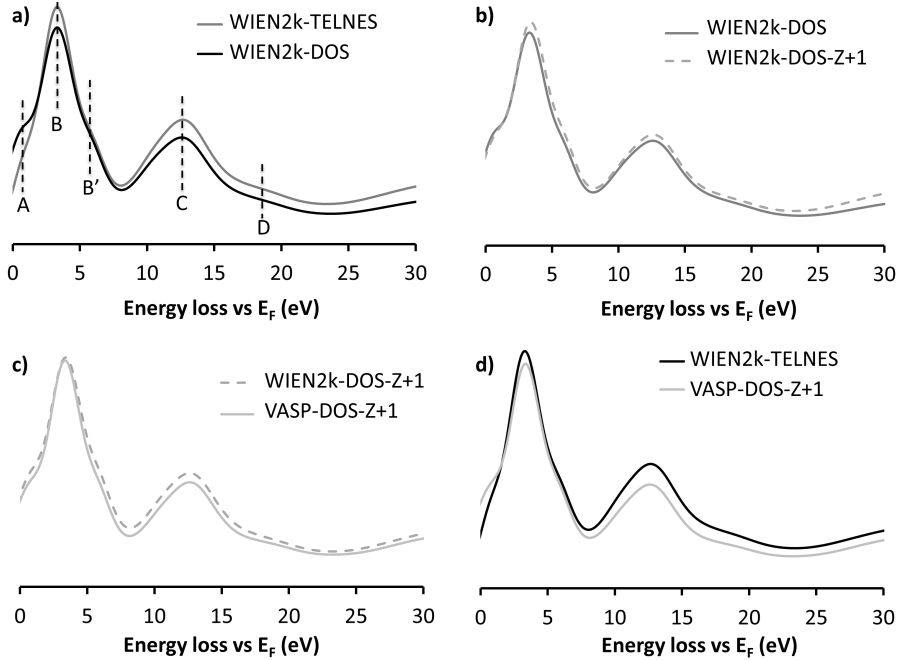


Figure S3: Effect of the various approximations described in the text on the simulation of the C-K edge in  $Ti_3C_2F_2$ . C-K edges obtained from (a) the explicit calculation of the inelastic cross section (WIEN2k-TELNES) or the C- $p$  DOS only (WIEN2k-DOS), (b) C- $p$  DOS considering a real core-hole (WIEN2k-DOS) or the Z+1 approximation (WIEN2k-DOS-Z+1), and (c) C- $p$  DOS in the Z+1 approximation computed in an all-electron/full potential approach (WIEN2k-DOS-Z+1) or using a PAW approach (VASP-DOS-Z+1). (d) Summary: comparison between the exact calculation of the C-K edge in a single particle approach (WIEN2k-TELNES) and the approach used in the paper (VASP-DOS-Z+1). Lines are given as guides to the eyes.

The effect of the approximations (i) to (iii) are illustrated in figure S3 (a) to (c) respectively. Figure S3(d) summarizes the comparison between the exact calculation (*i.e.* the evaluation of the inelastic cross section using WIEN2k) and the simulations presented in the paper (*i.e.* DOS calculations based on the PAW approach considering the Z+1 approximation). As evidenced in figure S3, the main approximation in our PAW calculation is to ignore the matrix elements in the calculations which slightly modifies the intensities of the fine structures compared the calculation based on the DOS (see figure S3-a). However, as evidenced in figure S3-d, such an approximation has clearly little effect on the overall simulations and our PAW-based calculations give very good results: all the fine structures are present at the very same energy with very comparable intensities when compared to the WIEN2k-TELNES calculations.

### 3 Effect of the mixing of T-groups on the C-K edge

In order to have an estimate of the effect of disorder and mixing between the -F, -OH and -O surface groups on the C-K edge, we average the contribution of the OH-type and O-type C-K edges for different compositions ranging from 10% to 90% in O. Given that -OH and -F give identical C-K edges, there is no need to take this last configuration into account in this approach. As evidenced in fig.S4-a, the averaging mainly results in a broadening of the first peak and an increase of the energy separation between peaks B and C (labelled  $\Delta E_{BC}$ ) when the -O content is increased. The evolution of  $\Delta E_{BC}$  at the C-K edge as a function of the O content is sketched in fig.S4-b. From the comparison between the theoretical values and the one deduced from experiments, the O-type terminations content is estimated to be below 20% (see fig.S4-b). The experimental positions of the structures B and C were extracted directly from the I(E) data (I being the recorded intensity and E the energy-loss). Given the very low noise level at the C-K edges, this procedure gives accurate energy positions.

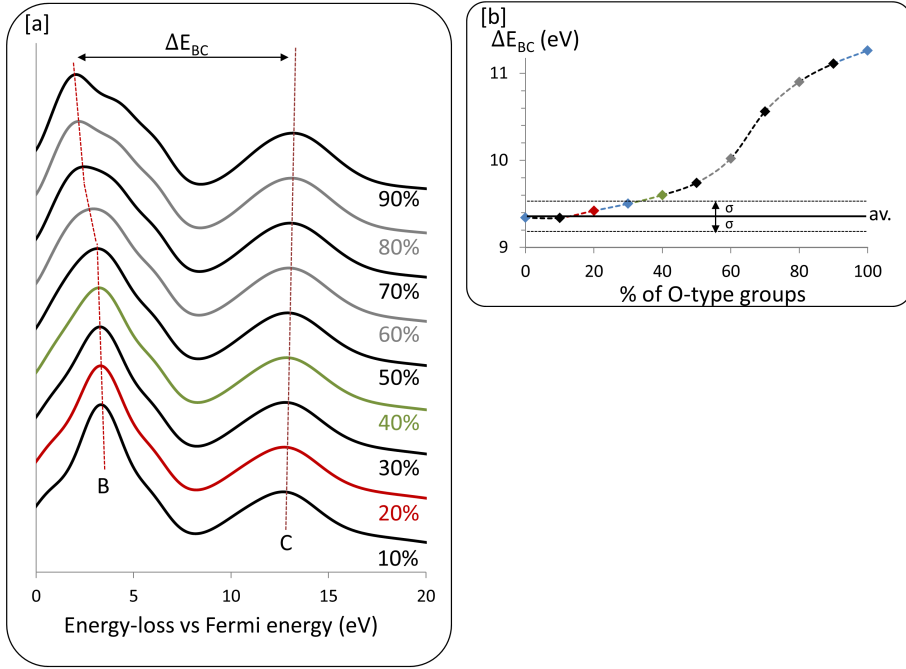


Figure S4: (a) Evolution of the ELNES at the C-K edge obtained by averaging the -OH and -O type C-K edges for different -O contents ranging from 10% to 90%. (b) Evolution of  $\Delta E_{BC}$  at the C-K edge as a function of the O content. The average value of 9.35 eV, obtained from 13 different experimental spectra, is represented by a thick black line. The standard deviation (0.2 eV) is given in dashed line. Lines are given as guides to the eyes.

The main approximation in this approach is to neglect the interaction be-

tween different T-groups. To investigate this last point, one approach could be to run calculations based on supercells. These calculations, beyond the scope of this paper, would however be very time-consuming for low -O amounts. Given that our simulations of the F-K edge give good results when compared to experiments, one can reasonably assume that the interactions between neighbouring T-groups are rather small.

## References

- [1] M. Ghidiu, M.R. Lukatskaya, M.-Q. Zhao, Y. Gogotsi and M.W. Barsoum, *Nature* **516**, 78 (2014)
- [2] M. Naguib, M. Kurtoglu, V. Presser, J. Lu, J. Niu, M. Heon, L. Hultman, Y. Gogotsi, M.W. Barsoum, *Adv. Mater.* **23**, 4248 (2011)
- [3] P. Blaha, K. Schwarz, G.K.H. Madsen, D. Kvaniscka, and J. Luitz, WIEN2k, an augmented plane wave+local orbitals program for calculating crystal properties, Technische Universität WIEN, Austria, 2001.
- [4] C. Hébert, *Micron* **38**, 12 (2007)
- [5] D. Magne, V. Mauchamp, S. Célérier, P. Chartier, and T. Cabioc'h, *Phys. Rev. B* **91**, 201409(R) (2015)